

Active vibration control: considering effect of electric field on coefficients of PZT patches

Sukesha Sharma^{*1}, Renu Vig¹ and Navin Kumar²

¹UIET, Panjab University, Chandigarh, India

²IIT Ropar, Punjab, India

(Received August 23, 2014, Revised November 28, 2015, Accepted November 30, 2015)

Abstract. Piezoelectric coefficient and dielectric constant of PZT-5H vary with electric field. In this work, variations of these coefficients with electric field are included in finite element modelling of a cantilevered plate instrumented with piezoelectric patches. Finite element model is reduced using modal truncation and then converted into state-space. First three modal displacements and velocities are estimated using Kalman observer. Negative first modal velocity feedback is used to control the vibrations of the smart plate. Three cases are considered v.i.z case 1: in which variation of piezoelectric coefficient and dielectric constant with electric field is not considered in finite element model and not considered in Kalman observer, case 2: in which variation of piezoelectric coefficient and dielectric constant with electric field is considered in finite element model and not considered in Kalman observer and case 3: in which variation of piezoelectric coefficient and dielectric constant with electric field is considered in finite element model as well as in Kalman observer. Simulation results show that appreciable amount of change would appear if variation of piezoelectric coefficient and dielectric constant with r.m.s. value of electric field is considered.

Keywords: active vibration control; finite element modelling; piezoelectric; Kalman; smart structure

1. Introduction

Technique of controlling structural vibrations by using external source of energy is called "Active Vibration Control" (AVC). Such structures exhibit desired dynamic characteristics even in presence of external load or changes in environment and are called smart structures (Cao *et al.* 1999). A smart structure (actively controlled structure) essentially consists of sensors to capture structural displacements, processor to manipulate sensor signal and actuators to bring about change in smart structure as per orders of the processor (Malgaca *et al.* 2009). In smart structures piezoelectric patches have been widely used as sensors as well as actuators. Piezoelectric materials have coupled electromechanical properties. When mechanical stress is applied on a piezoelectric material, electrical voltage is generated and when electrical voltage is applied across a piezoelectric material, mechanical strain is produced. Electromechanics of piezoelectric materials is expressed in form of constitutive equations (ANSI/IEEE std. 1987, Cady 1964, Ikeda 1996). Stress and electric displacement developed in a piezoelectric material are also dependent on

*Corresponding author, E-mail: sukeshaiet@gmail.com

variables such as temperature, electric field, humidity (moisture), age, hysteresis etc (Apte and Ganguly 2009, Birman 2005, Smittakorn and Heyliger 2000, Wang *et al.* 1998). Piezoelectric coefficient and dielectric constant of piezoelectric materials vary with change in these parameters. Active vibration control of a cantilevered plate instrumented with piezoelectric patches can be made robust to variations in temperature by considering variation of piezoelectric coefficient and permittivity with temperature in Kalman observer (Gupta *et al.* 2011, Gupta *et al.* 2012). Piezoelectric coefficient and dielectric constant primarily determine applicability of a piezoelectric material as a sensor or an actuator. These constants also vary with change in electric field (Apte and Ganguly 2009, Wang *et al.* 2003, Zhang *et al.* 1995). A piezoelectric sensor or an actuator would not perform as expected if variation in values of piezoelectric coefficient and dielectric constant with electric field is ignored.

Permittivity and relative amplitudes of piezoelectric coefficient ' d_{31} ' increases with increase in applied electric field for PZT-5H (Kugal and Cross 1998, Masys *et al.* 2003, Sirohi and Chopra 2000). Relative change in ' d_{31} ' i.e. ' K_1 ' of PZT-5H piezoelectric ceramic can be expressed as a function of r.m.s value of applied AC electric field \tilde{E} (kv/cm) as (Apte and Ganguly 2009)

$$K_1 = 1 + 0.1013 \tilde{E} + 0.4125 \tilde{E}^2 - 0.3928 \tilde{E}^3 + 0.1313 \tilde{E}^4 \quad (1.1)$$

Similarly percent increase in dielectric constant (permittivity) i.e., ' K_e ' can be expressed as (Apte and Ganguly 2009)

$$K_e = 7.32 - 5.9754 \tilde{E} + 5.3187 \tilde{E}^2 \quad (1.2)$$

In a smart structure, actuators deform the host structure as per control law. For control laws based upon full state feedback knowledge of all the states is required. Many times full state is constructed from time response of limited number of sensors using Kalman observer. Responses of a piezoelectric actuator and sensor of a smart structure would be wrongly calculated if variation of piezoelectric coefficient and permittivity with electric field is ignored in Kalman observer. There is no work in literature where in variation of piezoelectric coefficient and permittivity with electric field has been considered in structural vibration control of structures using piezoelectric patches. Work done in AVC is without considering variation of piezoelectric coefficient and permittivity with electric field (Bruant *et al.* 2001, Hu *et al.* 2007, Hu 2012, Kim *et al.* 2013, Li *et al.* 2014, Lin and Huang 1999, Lin and Chan 2013, Li and Narita 2014, Raja *et al.* 2002, Sharma *et al.* 2005, Shin *et al.* 2013, Zabihollah 2007, Zhang *et al.* 2013). There are numerous works in which finite element method has been employed to create a mathematical model of smart structure instrumented with piezoelectric patches and Kalman observer has been employed to estimate states of the smart structure. In all these works, variation of piezoelectric coefficient and permittivity with electric field has been ignored. In present work, structural vibrations of a cantilevered square plate instrumented with piezoelectric sensor and piezoelectric actuator have been controlled using finite element model and Kalman observer which consider variation of piezoelectric coefficient and permittivity with electric field. Finite element method based upon Hamilton's principle has been used to create a mathematical model. Modal truncation has been used to reduce the model considering only first three modes of vibration. This reduced model has then been converted into a state space model. Kalman observer having knowledge of variation of piezoelectric coefficient and permittivity with electric field has been used to estimate all the states of the system. Traditionally, control matrix and sensor vector used in the Kalman observer are taken invariant with respect to electric field. Present work proposes a novel technique in which control matrix and sensor vector of the Kalman observer are made electric-field dependent. Thereafter, negative first modal velocity

feedback has been used to control the structural vibrations of the smart structure. Newmark- β method has been used to solve system of coupled second order ordinary differential equations. Section-2 presents finite element modelling of a smart plate considering variation of piezoelectric coefficient ‘ d_{31} ’ and dielectric constant ‘ ϵ_{33} ’ with respect to r.m.s. value of electric field. Section-3 has simulation results and in section-4 conclusions are drawn.

In simulations three distinct cases are possible and therefore have been presented. Case 1 presents simulations such that variation of piezoelectric coefficient and permittivity with electric field is ignored in finite element model as well as in Kalman observer. This case presents simulations of smart piezostructure as being done as of now by researchers worldwide. Case 2 presents simulations such that variation of piezoelectric coefficient and permittivity with electric field is considered in finite element model and ignored in Kalman observer. Case 3 presents simulations such that variation of piezoelectric coefficient and permittivity with electric field is included in finite element model as well as in Kalman observer.

2. Mathematical modelling of the smart plate

Consider a cantilevered square plate of length 16 cm, width 16 cm and thickness 0.6 mm as shown in Fig. 1. Plate is instrumented with a piezoelectric sensor-actuator pair, polarized in thickness direction. The top and bottom surface of each piezoelectric is covered by electrodes. At the device location, structure is composite in thickness direction, with two piezoelectric and one elastic layer. The arbitrary quadrilateral bending element of plate is adopted in this work for finite element formulation and the plate is divided into 64 elements having 81 nodes. Fig. 2 shows the element with four node points, one at each corner. At each node three degrees of freedom are considered v.i.z displacement ‘ w ’ normal to the plate and two rotations θ_x and θ_y . Constitutive equations of piezoelectricity in e-form can be written as

$$D_n = e_{nkl} \epsilon_{kl} + \epsilon_{nm} E_m \tag{2.1}$$

$$\sigma_{kl} = c_{ijkl} \epsilon_{ij} - e_{nkl} E_n \tag{2.2}$$

where ‘ D_n ’ is electric displacement in ‘ n^{th} ’ direction, ‘ e_{nkl} ’ is piezoelectric stress coefficient, ‘ ϵ_{kl} ’ is shear strain in ‘ l^{th} ’ direction in plane perpendicular to the ‘ k^{th} ’ direction, ‘ ϵ_{nm} ’ is permittivity coefficient, ‘ σ_{kl} ’ is stress in ‘ l^{th} ’ direction in plane perpendicular to ‘ k^{th} ’ direction, ‘ c_{ijkl} ’ is coefficient of elasticity, ‘ E_m ’ is electric field in ‘ m^{th} ’ direction and ‘ E_n ’ is electric field in ‘ n^{th} ’ direction. Here ‘ ij ’ & ‘ kl ’ varies from 1 to 6 and ‘ n ’ & ‘ m ’ varies from 1 to 3. For thin plate, $\epsilon_3 = 0, \epsilon_4 = 0$ and $\epsilon_5 = 0$. In present case electric field is applied only in 3rd direction therefore $E_1 = 0$ and $E_2 = 0$. Some piezoelectric stress coefficients are zero and $e_{31} = e_{32}$ for PZT-5H.

Value of piezoelectric coefficients and permittivity of PZT-5H changes with change in r.m.s value of applied electric field. To incorporate this fact in Eqs. (2.1) and (2.2) let us take $e_{31} = \bar{e}_{31} + \widetilde{e}_{31}$, where ‘ \bar{e}_{31} ’ is the initial value of the piezoelectric coefficient at zero electric field and ‘ \widetilde{e}_{31} ’ is increment in value of the piezoelectric coefficient as electric field increases. ‘ \widetilde{e}_{31} ’ is function of r.m.s value of applied electric field and can be written using constants ‘ a_1 ’ and ‘ a_2 ’ as

$$\begin{aligned} \widetilde{e}_{31} &= a_1 E_{rms} + a_2 E_{rms}^2, \text{ i.e} \\ e_{31} &= \bar{e}_{31} + \widetilde{e}_{31} = \bar{e}_{31} + (a_1 E_{rms} + a_2 E_{rms}^2) \end{aligned} \tag{2.3}$$

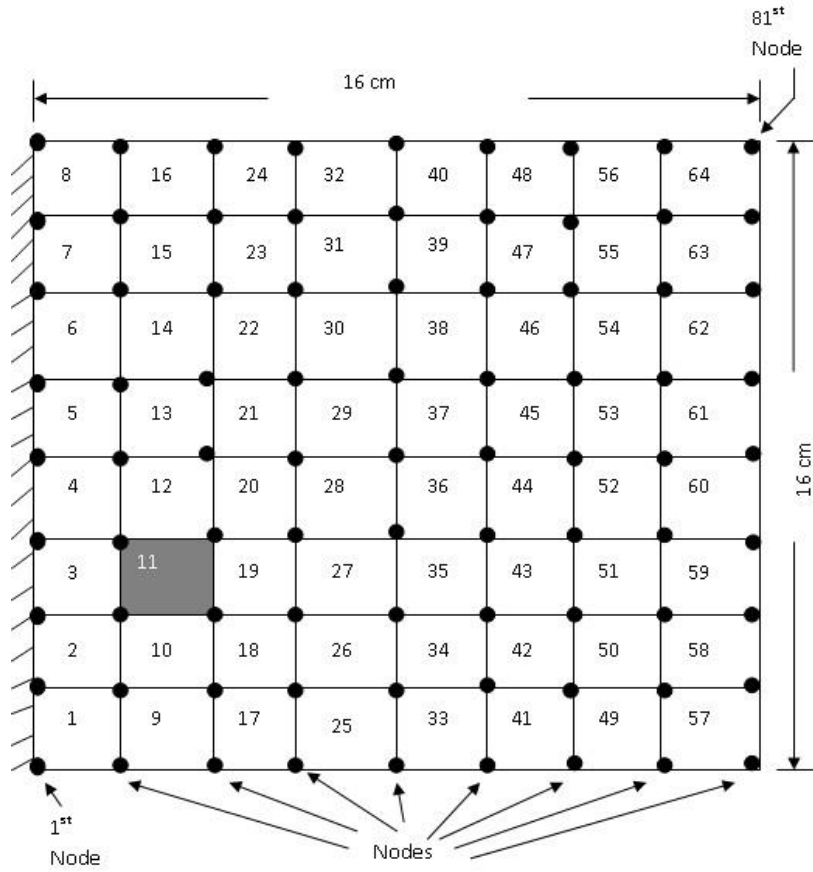


Fig. 1 Cantilevered smart plate

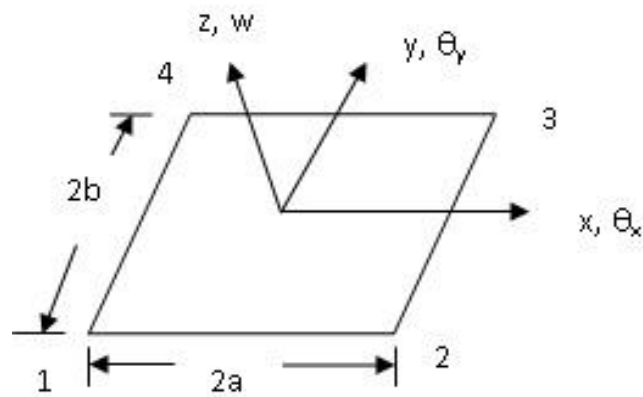


Fig. 2 Quadrilateral plate element

Similarly using constants ‘ a_3 ’ and ‘ a_4 ’

$$\epsilon_{33} = \overline{\epsilon}_{33} + \widetilde{\epsilon}_{33} = \overline{\epsilon}_{33} + (a_3 E_{rms} + a_4 E_{rms}^2) \tag{2.4}$$

where ‘ $\overline{\epsilon}_{33}$ ’ is value of permittivity at zero electric field and ‘ $\widetilde{\epsilon}_{33}$ ’ is increment in value of permittivity as electric field increases. For PZT-5H numerical value of ‘ a_1 ’ is $-4.6e-05$, ‘ a_2 ’ is $-1.8e-10$, ‘ a_3 ’ is $6.4e-14$, ‘ a_4 ’ is $6.11e-20$ and is obtained from graph of variation of piezoelectric coefficient ‘ e_{31} ’ and dielectric constant ‘ ϵ_{33} ’ w.r.t. electric field (Apte and Ganguly 2009).

Substituting values of ‘ e_{31} ’ and ‘ ϵ_{33} ’ in Eqs. (2.1) and (2.2), we get

$$\{D\}_{3 \times 1} = [e_1]_{3 \times 3} \{\epsilon\}_{3 \times 1} + [\epsilon_1]_{3 \times 1} E_3 \tag{2.5}$$

$$\{\sigma\}_{3 \times 1} = [C]_{3 \times 3} \{\epsilon\}_{3 \times 1} - [e_2]_{3 \times 1} E_3 \tag{2.6}$$

Where $[e_1] = \begin{bmatrix} 0 & 0 & 0 \\ 0 & 0 & 0 \\ (\overline{e}_{31} + a_1 E_{rms} + a_2 E_{rms}^2) & (\overline{e}_{31} + a_1 E_{rms} + a_2 E_{rms}^2) & 0 \end{bmatrix}$,

$[\epsilon_1] = \begin{bmatrix} 0 \\ 0 \\ (\overline{\epsilon}_{33} + a_3 E_{rms} + a_4 E_{rms}^2) \end{bmatrix}$, $[e_2] = \begin{bmatrix} (\overline{e}_{31} + a_1 E_{rms} + a_2 E_{rms}^2) \\ (\overline{e}_{31} + a_1 E_{rms} + a_2 E_{rms}^2) \\ 0 \end{bmatrix}$,

$[C] = \begin{bmatrix} C_{11} & C_{12} & 0 \\ C_{12} & C_{22} & 0 \\ 0 & 0 & C_{66} \end{bmatrix}$

Applying Hamilton’s principle to smart plate shown in Fig. 1 and solving further we get equation of motion of one finite element (Gupta *et al.* 2011, Petyt 1998). As shown in Fig. 1, cantilevered plate has 64 elements and 81 nodes. Nine nodes lying on the cantilevered edge of the plate can not experience any displacement or rotation. Transverse displacement, rotation about x-axis and rotation about y-axis are experienced by each of the remaining 72 nodes. Therefore, cantilevered plate has 216 degrees of freedom ($3 \times 72 = 216$). Following the assembly procedure, global equations of motion can be expressed as

$$[M]_{216 \times 216} \{\ddot{x}\}_{216 \times 1} + [C]_{216 \times 216} \{\dot{x}\}_{216 \times 1} + [K]_{216 \times 216} \{x\}_{216 \times 1} = \{F\}_{216 \times 1} \tag{2.7}$$

where ‘ $[M]$ ’ is mass matrix, ‘ $[C]$ ’ is damping matrix, ‘ $[K]$ ’ is stiffness matrix and ‘ $\{x\}$ ’ is displacement vector. ‘ $\{F\}$ ’ is force vector and consists of ‘ $\{F_1\}$ ’ which is the force applied by a piezoelectric actuator at element number 11 and is given as

$$\{F_1\} = [k_{uv}^e] [k_{vv}^e]^{-1} Q_{ext} \tag{2.8}$$

where

$[k_{uv}^e] = -\int_p \frac{z}{2d} [B_u]^T [e_2] d\tau - \int_p \frac{z}{2} [B_u]^T [e_1]^T \{B_v\} d\tau$, is the electromechanical interaction matrix.

$$[k_{vv}^e] = \int_p \frac{1}{d} \{B_v\}^T [\epsilon_1] d\tau, \quad [B_u] = -\left\{ \frac{\partial^2}{\partial x^2} \quad \frac{\partial^2}{\partial y^2} \quad 2 \frac{\partial^2}{\partial x \partial y} \right\}^T [N]$$

$$Q_{ext} = \int_{A_p} q dA_p, \quad \{E\} = -\{0 \quad 0 \quad 1/d\}^T v = -\{B_v\} v.$$

where subscript 'p' refers to piezoelectric patch, ' A_p ' is the surface area of piezoelectric patch, ' $[N]$ ' is Hermite's interpolation shape function, ' q ' is charge, ' d ' is thickness of piezoelectric patch and ' v ' is the voltage. Matrix Eq. (2.7) has coupled second order ordinary differential equations. These equations can be uncoupled using following modal transformation.

$$\{x\}_{216 \times 1} = [U]_{216 \times 3} \{\eta\}_{3 \times 1} \quad (2.9)$$

where ' $[U]_{216 \times 3}$ ' is orthonormal modal matrix and ' $\{\eta\}_{3 \times 1}$ ' is a vector of first three vibration modes. In state space, modal equations of the smart plate can be written as

$$\{\dot{s}\} = [A]\{s\} + [B]V_{control} \quad (2.10)$$

where 'A' is system matrix, 'B' is control matrix and ' $\{s\}$ ' is given as

$$\{\dot{s}\} = \{\dot{\eta}_1 \ \dot{\eta}_2 \ \dot{\eta}_3 \ \ddot{\eta}_1 \ \ddot{\eta}_2 \ \ddot{\eta}_3\}_{6 \times 1}^T \quad (2.11)$$

In this work, first modal displacement is controlled by taking first modal force proportional to negative of first modal velocity, i.e

$$f_1 \propto -\dot{\eta}_1 \quad (2.12)$$

External voltage applied on the piezoelectric actuator is therefore calculated as (Baz 1988, Sharma *et al.* 2007)

$$V_{control} = \frac{-g \eta_1}{\{[U]^T \{f_c\} Z_{actuator}\}_{1,1}} \quad (2.13)$$

where $f_c = [k_{uv}^e][k_{vv}^e]^{-1}$, ' $Z_{actuator}$ ' is capacitance of actuator and ' g ' is the gain of simple negative velocity feedback which is taken by hit and trial method. Present work uses first modal velocity in control law which can be either measured or estimated. Measurement of modal velocity is difficult as it requires special type of modal sensors (Friswell 2003, Zenz *et al.* 2013). In this work entire state vector is estimated using one piezoelectric sensor and Kalman observer. Thereafter, first modal velocity has been picked from estimated state vector so as to be used in the control law. Estimated state vector ' $\{s_e\}$ ' is given by (Gopal 2010)

$$\{s_e\}_{6 \times 1} = [dA]_{6 \times 6} \{s_e\}_{6 \times 1} + [dB]_{6 \times 1} V_{control} + \{L_{kal}\}_{6 \times 1} (V_{sensor} - \{C_{sensor}\}_{1 \times 6} \{s_e\}_{6 \times 1}) \quad (2.14)$$

$$\{s_e\}_{6 \times 1} = \{s_e\}_{6 \times 1} + \{M_{kal}\}_{6 \times 1} (V_{sensor} - \{C_{sensor}\}_{1 \times 6} \{s_e\}_{6 \times 1}) \quad (2.15)$$

where $[dA]$ and $[dB]$ are discrete forms of 'A' and 'B' matrices. ' $\{M_{kal}\}$ ' and ' $\{L_{kal}\}$ ' are Kalman gain matrices. $C_{sensor} = -[k_{vv}^e]^{-1}[k_{vu}^e]$ and ' V_{sensor} ' is the sensor voltage. Matrix $[dB]$ and vector C_{sensor} are dependent upon matrices $[k_{uv}^e]$ and $[k_{vv}^e]$. From Eq. (2.8) it is clear that $[k_{uv}^e]$ and $[k_{vv}^e]$ are dependent on piezoelectric coefficient and permittivity. Kalman observer in case 3 considers electric field dependence of piezoelectric coefficient and permittivity in Eqs. (2.14) and (2.15), whereas Kalman observer in case 1 and case 2 ignores this fact.

2.1 Comparison of control voltages applied by case 2 and case 3 control for a given control gain and a given initial condition

Control voltage applied on the actuator has dependence on factors as shown below:

$$V_{control} \propto \frac{-\eta_1}{\{[U]^T \{f_c\} Z_{actuator}\}_{1,1}}$$

As used in Eq. (2.13), $\{f_c\} = [k_{uv}^e][k_{vv}^e]^{-1}$

Substituting values of $[k_{uv}^e]$ and $[k_{vv}^e]$ from Eq. (2.8), we get for case 3:

$$V_{control_case3} \propto \frac{-\eta_1}{\{[U]^T \left(-\int_p \frac{z}{2d} [B_u]^T [e_2] d\tau - \int_p \frac{z}{2} [B_u]^T [e_1]^T \{B_v\} d\tau \right) \left(\int_p \frac{1}{d} \{B_v\}^T [\epsilon_1] d\tau \right) Z_{actuator} \}_{1,1}}$$

Substituting values of $[e_2]$, $[e_1]$ and $[\epsilon_1]$ from Eqs. (2.5) and (2.6), we get case 3 voltage:

$$V_{control_case3} \propto \frac{-\eta_1}{\left\{ [U]^T \left(\left(-\int_p \frac{z}{2d} [B_u]^T \begin{bmatrix} (\overline{e}_{31} + a_1 E_{rms} + a_2 E_{rms}^2) \\ (\overline{e}_{31} + a_1 E_{rms} + a_2 E_{rms}^2) \\ 0 \end{bmatrix} d\tau \right) \left(\int_p \frac{1}{d} \{B_v\}^T \begin{bmatrix} 0 \\ 0 \\ (\overline{\epsilon}_{33} + a_3 E_{rms} + a_4 E_{rms}^2) \end{bmatrix} d\tau \right) \right\} Z_{actuator} \right\}_{1,1}}$$

From above relation it can be easily reasoned that for case 3 control

$$V_{control_case3} \propto \frac{1}{(C_1 \overline{e}_{31} + C_2 a_1 E_{rms} + C_3 a_2 E_{rms}^2)(C_4 \overline{\epsilon}_{33} + C_5 a_3 E_{rms} + C_6 a_4 E_{rms}^2)} \tag{2.16}$$

whereas for case 2 control

$$V_{control_case2} \propto \frac{1}{(\overline{e}_{31})(\overline{\epsilon}_{33})} \tag{2.17}$$

where C_1, C_2, C_3, C_4, C_5 and C_6 are constants. η_1 initially for both case 2 and case 3 control is almost same for same initial condition. It can be seen from Eqs. (2.16) and (2.17) that for a given control gain and a given initial condition ‘ $V_{control_case3}$ ’ will be lesser than ‘ $V_{control_case2}$ ’. As a result, for a given control gain and given initial condition more actuation moments will be applied by case 2 control resulting in more vibration suppression in case 2 control.

2.2 Controllability and observability test

1. Necessary and sufficient condition for the system to be completely controllable is that $n \times n$ controllability matrix, $U = [B \ AB \ A^2B \ \dots \ A^{n-1}B]$ has rank equal to n , where ‘ A ’ is system matrix and ‘ B ’ is control matrix (Gopal 2010). In this system controllability matrix size is 6×6 and it has rank equal to 6. Hence this system is completely controllable.
2. Necessary and sufficient condition for the system to be completely observable is that $n \times n$ observability matrix, $V = [C \ CA \ CA^2 \ \dots \ CA^{n-1}]^T$ has rank equal to n , where ‘ A ’ is system matrix and ‘ C ’ is output matrix (Gopal 2010). In this system observability matrix size is 6×6 and it has rank equal to 6. Hence this system is completely observable.

2.3 Stability

The present system being a mechanical structure has inherent structural damping ratio of 0.004. In present work negative first modal velocity feedback has been employed to control the structural vibrations. Usage of this control law is well known to be stable as it further increases system damping. All the roots of characteristic equation of closed loop transfer function are in left half of the complex plane (for controlled as well as uncontrolled response).

3. Simulations and results

Cantilevered plate of size 16 cm \times 16 cm \times 0.6 mm is considered and this plate is divided into 64 finite elements as shown in Fig. 1. Plate is equipped with two piezoelectric patches in collocated fashion at element no. 11, one above and one below the plate. Material properties of host structure and piezoelectric patch are tabulated in Table (1). Using finite element procedures as detailed in section 2, a system of 216 second order ordinary differential coupled equations is obtained. These coupled equations are solved using Newmark- β method. Kalman observer is used to estimate first three modes of the plate in time domain. Modal force in first mode is taken proportional to negative of modal velocity of first mode. Simulations are divided into sections as: In section 3.1 free edge of the plate is disturbed with initial displacement of 1.1 mm for collocated sensor actuator pair at element number 11. In section 3.2 harmonic disturbance is given to plate through one actuator at element number 14 for collocated sensor actuator pair at element number 11. In section 3.3 free edge of the plate is disturbed with initial displacement of 1.1 mm with concurrent sensing at element number 11. In section 3.4 harmonic disturbance is given to plate through one actuator at element number 14 with concurrent sensing at element number 11.

3.1 Response to initial displacement (collocated sensor-actuator pair)

Cantilevered plate as shown in Fig. 1 is considered in which a piezoelectric sensor patch is instrumented on top surface of plate over entire element no 11 and a piezoelectric actuator patch is instrumented on bottom surface of plate below entire element no 11. Fig. 3 shows time response of first modal displacement when edge opposite to cantilevered edge of smart plate is given initial displacement of 1.1 mm and is controlled by simple negative first modal velocity feedback. As explained in last paragraph of 'introduction', three distinct cases of simulation are possible. Decay curve of case 1 has damping ratio of 0.015 and that of case 2 has damping ratio of 0.032. Decay curve of case 3 with damping ratio of 0.015 overlaps with that of case 1. This implies that a researcher who ignores variation of piezoelectric coefficient and permittivity with electric field will obtain the same decay curve in simulations as obtained by researcher who considers this variation in simulations. This result is attributed to the control law which applies same modal forces on the structure as there is no error between Kalman observer and finite element model (in case 1 and case 3). It has to be observed here that although due to no error between Kalman observer and finite element model (in case 1 and case 3) same modal forces get applied on the structure but the control voltages are different (in case 1 and case 3). Fig. 4 shows time response of control voltage applied on the actuator. It can be clearly seen that for a given gain of the negative velocity feedback, a researcher who ignores variation of piezoelectric coefficient and permittivity with electric field will predict larger control voltages. On the other hand researcher who considers these variations in finite element model as well as in Kalman observer, will obtain lesser control voltages.

Table 1 Material properties of host structure and piezoelectric patch

Property	Host structure	Piezoceramic (PZT-5H)
Density (kg/m ³)	7800	7500
Young's Modulus (N/m ²)	2.07×10^{11}	6.76×10^{10}
Poisson's ratio	0.3	0.3
Dielectric constant	-	3200
Length (m)	0.16	0.02
Width (m)	0.16	0.02
Thickness (m)	0.0006	0.00106

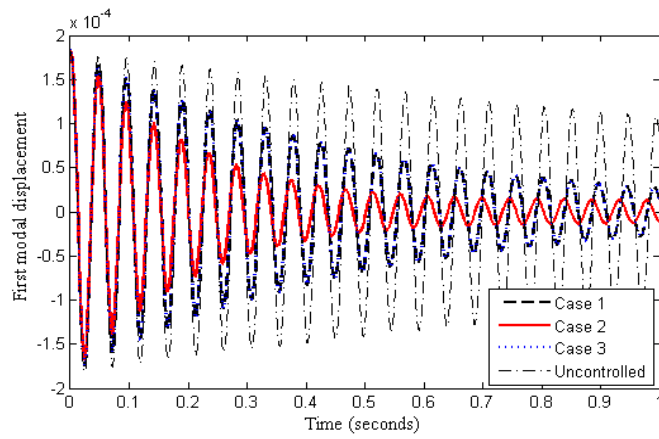


Fig. 3 Time response of first modal displacement when plate is controlled using negative modal velocity feedback

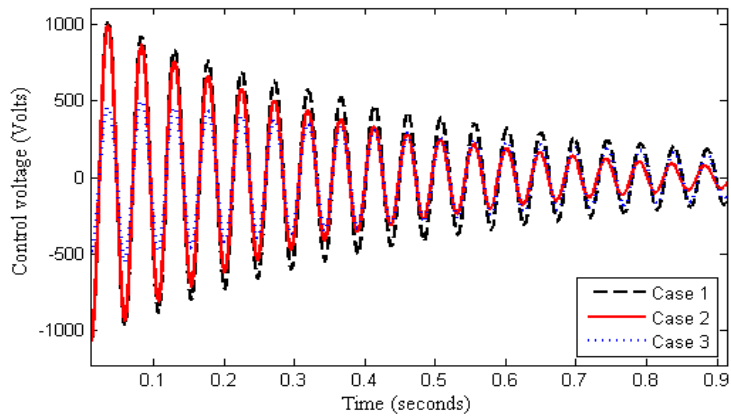


Fig. 4 Time response of control voltage when plate is controlled using negative modal velocity feedback

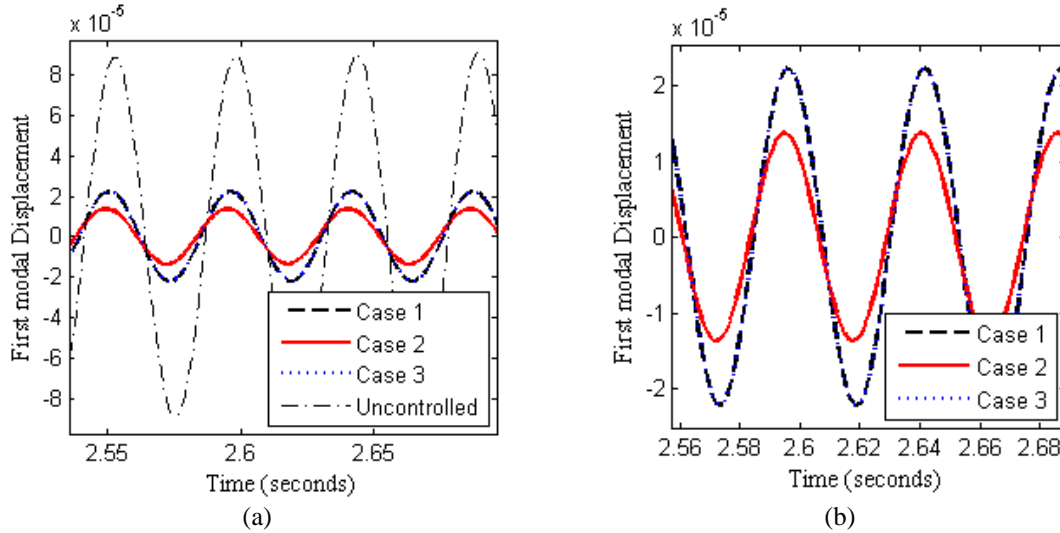


Fig. 5 (a) Time response of first modal displacement (harmonic disturbance) and (b) Comparison of case 1 controlled, case 2 controlled and case 3 controlled responses (zoomed part of Fig. 5 (a))

3.2 Response to harmonic disturbance (collocated sensor-actuator pair)

In this case two piezoelectric patches are pasted in collocated fashion over/below location of element no 11 and one piezoelectric actuator is pasted over location of element no 14 for providing harmonic disturbance to the plate. Fig. 5 shows time response of first modal displacement when smart plate is disturbed by a harmonic disturbance with frequency that of first mode. Again, first modal displacement is suppressed more in case 2 control than case 3 control and modal displacement of case 1 overlaps with that of case 3. Fig. 6 shows time-response of control voltage applied on the actuator when plate is disturbed by harmonic disturbance with frequency that of first mode. Voltages applied in case 1 are greater than that applied in case 2 and voltages applied in case 2 are greater than that applied in case 3. It is worth noting that although voltages applied in case 1 are largest but still the modal displacement in case 1 is not least. This is due to the fact that in case 3 and case 2 both piezoelectric coefficient and permittivity increase with increase in electric field resulting in more net actuation force applied by actuator per unit applied control voltage.

3.3 Response to initial displacement (Concurrent sensing)

In this case same piezoelectric patch is used for sensing as well as actuation (concurrent sensing) i.e., only one piezoelectric patch is instrumented over location of element number 11. Edge of the plate opposite to the cantilevered edge is given initial displacement of 1.1 mm. Fig. 7 gives time response of first modal displacement in open loop (uncontrolled response) and closed loop. It can be seen in Fig. 7 that damping ratio of uncontrolled response is 0.0040, of case 1 controlled response is 0.015, of case 2 controlled response is 0.021 and of case 3 controlled response is 0.015. Decay curve of modal displacement in case 1 overlaps with that in case 3. Fig. 8

shows time response of control voltage in case 1, case 2 and case 3. Control voltages applied in case 1 are larger than that applied in case 2 and case 3. It is clear from figure that upto about 0.4 seconds control voltage in case 2 is greater than that in case 3. After 0.4 seconds control voltage in case 3 is greater than that in case 2. This behaviour is attributed to the fact that in initial time upto 0.4 seconds electric-field on actuator is large and therefore appreciably increases d_{31} and ϵ_{33} of the actuator. Therefore upto 0.4 seconds lower voltages are applied in case 3.

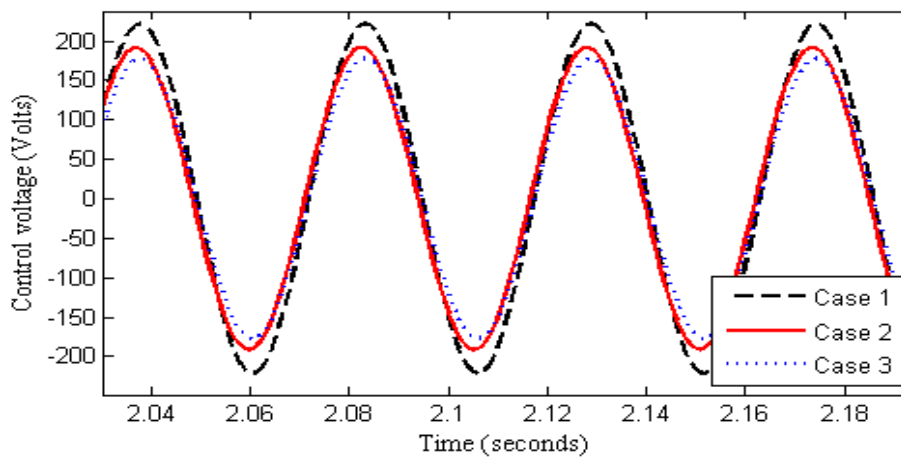


Fig. 6 Time response of control voltage (harmonic disturbance)

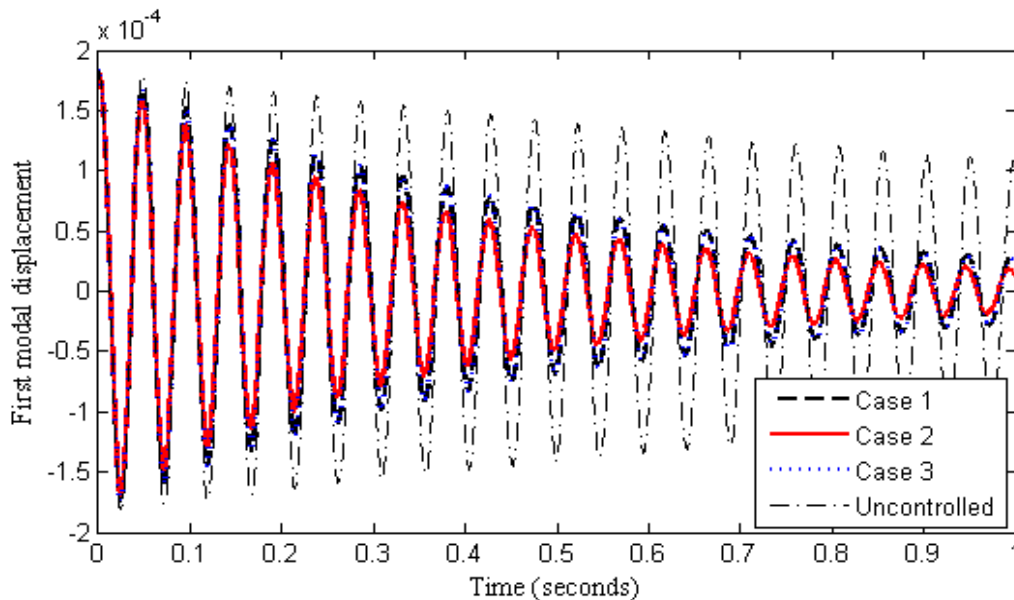


Fig. 7 Time response of first modal displacement when plate is controlled using negative modal velocity feedback (concurrent sensing)

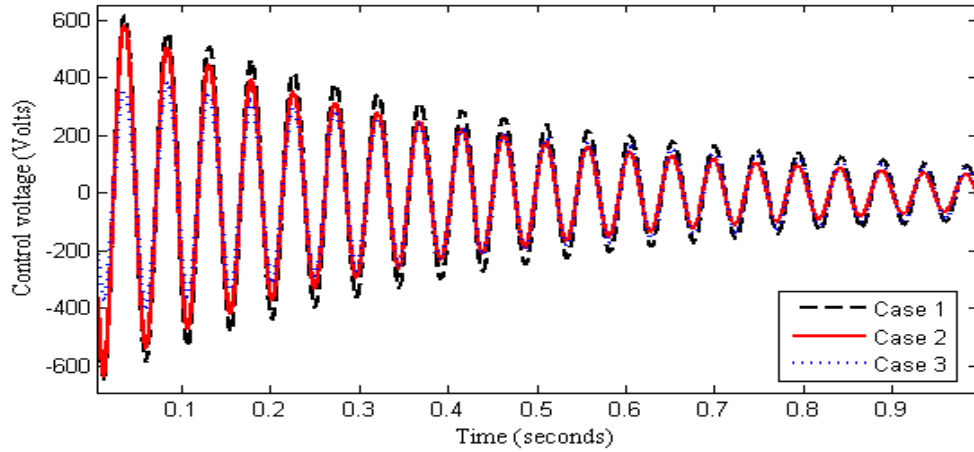


Fig. 8 Time response of control voltage for concurrent sensing when smart plate is disturbed by initial displacement of 1.1 mm

3.4 Response to harmonic disturbance (concurrent sensing)

Fig. 9 shows time response of first modal displacement when smart plate is disturbed by a harmonic disturbance with frequency that of first mode and controlled using a concurrent sensor at element number 11. Similar to previous study on harmonic disturbance, modal displacement in case 1 overlaps with that in case 3 and modal displacement in case 2 is suppressed more than that in case 3/case1. From Fig. 10 it is evident that voltages applied in case1 are greater than that in case2 and voltages applied in case2 are greater than that in case3.

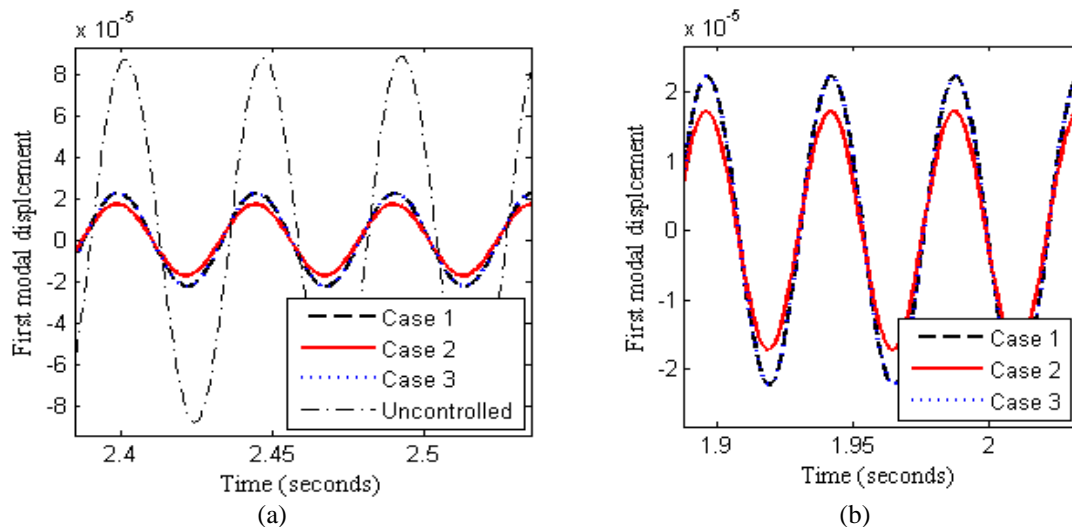


Fig. 9 (a) Time response of first modal displacement (harmonic disturbance and concurrent sensing) and (b) Comparison of case 1, case 2 and case 3 controlled response (zoomed part of Fig. 9 (a))

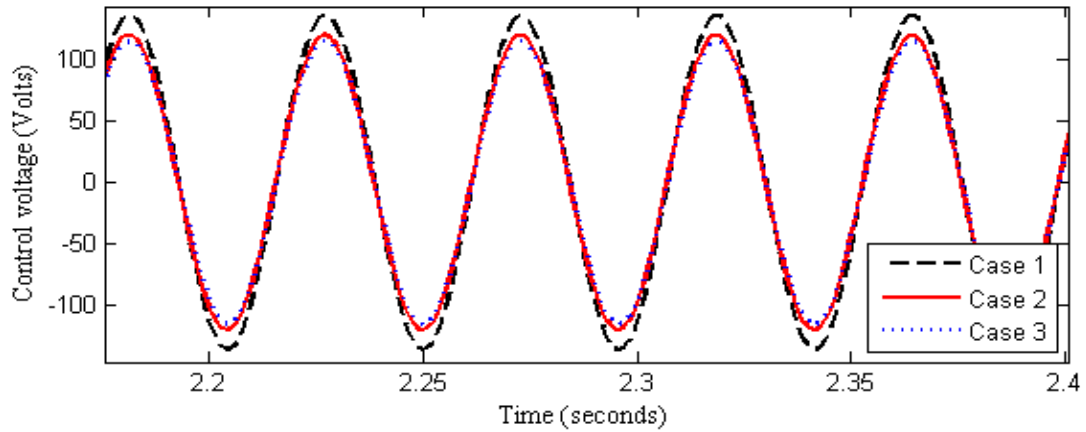


Fig. 10 Time response of control voltage in case of harmonic disturbance and concurrent sensing

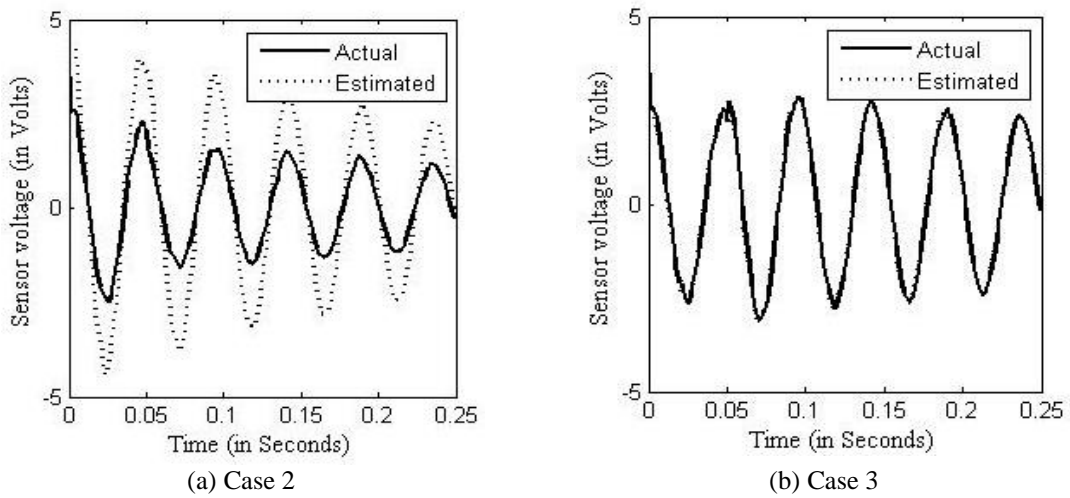


Fig. 11 Comparison of actual and estimated sensor voltage

3.5 Comparison of sensor voltage (in case of initial displacement of 1.1 mm, non-concurrent sensing)

Fig. 11 shows time response of actual sensor voltage and estimated sensor voltage in case 2 control and case 3 control. Actual sensor voltage almost matches with estimated sensor voltage in case 3 (Fig. 11(b)) and there is considerable difference between actual and estimated sensor voltage in case 2 (Fig. 11(a)).

4. Conclusions

This work considered a cantilevered plate instrumented with piezoelectric patches. Constitutive equations of piezoelectricity were modified by including the variation of piezoelectric coefficient and permittivity with r.m.s value of applied electric field. Using these modified constitutive equations, a finite element model of thin plate was derived systematically using Hamilton's principle. FE model was reduced using modal truncation, converted into state space model and simple negative first modal velocity feedback was used as control approach. For a given initial displacement/harmonic disturbance given to smart plate and a given gain of negative velocity feedback, it can be concluded that:

- Time response of first modal displacement obtained by completely ignoring variation of piezoelectric coefficient and permittivity with electric field, overlaps with that obtained by considering this variation in finite element model and Kalman observer. Important difference is that lesser control voltages get applied in the latter case.
- If variation of piezoelectric coefficient and permittivity with electric field is completely ignored then vibration suppression is less than the case when this variation is considered in finite element model and ignored in Kalman observer. Lesser control voltages get applied in the latter case.
- In active vibration control, appreciable amount of difference appears in simulations if variation of piezoelectric coefficient and dielectric constant w.r.t. electric field is considered.

References

- ANSI/IEEE Std 176-1987 (1988), IEEE Standard on Piezoelectricity.
- Apte, D.A. and Ganguli, R. (2009), "Influence of temperature and high electric field on power consumption by piezoelectric actuated integrated structure", *Comput. Mat. Cont.*, **329**(1), 1-23.
- Baz, A. and Poh, S. (1988), "Performance of an active control system with piezoelectric actuators", *J. Sound Vib.*, **126**(2), 327-343.
- Birman, V. (2005), Physically nonlinear behaviour of piezoelectric actuators subject to high electric fields, final report, US army research, Feb.
- Bruant, I., Coffignal, G., Lene, F. and Verge, M. (2001), "Active control of beams structures with piezoelectric actuators and sensors: modeling and simulation", *Smart Mater. Struct.*, **10**(2), 404-408.
- Cady, W.G. (1964), *Piezoelectricity*, vol 1, Dover Publications, New York.
- Cao, W., Cudney, H. and Waser, R. (1999), "Smart materials and structures", *Proc. National Acad. American Sci. USA*, **96**, 8330-8331.
- Friswell, M. (2003), "Modal sensors and actuators for beam and plate structures", *Smart Struct. Mat.*, **5050**, 92-100.
- Gopal, M. (2010), *Digital Control and State Variable Methods*, (3rd Ed.), Tata McGraw Hill, New Delhi.
- Gupta, V., Sharma, M. and Thakur, N. (2012), "Active structural vibration control: robust to temperature variations", *Mech. Syst. Signal. Pro.*, **33**, 167-180.
- Gupta, V., Sharma, M. and Thakur, N. (2011), "Active vibration control of a smart plate using a piezoelectric sensor-actuator pair at elevated temperatures", *Smart Mater. Struct.*, **20**, 105023-1 – 105023-13.
- Gupta, V., Sharma, M. and Thakur, N. (2011), "Mathematical modeling of actively controlled piezo smart structures: A review", *Smart Struct. Syst.*, **8**(3), 275-302.
- Hu, J. (2012), "Vibration control of smart structure using sliding mode control with observer", *J. Comput.*,

- 7(2), 411-418.
- Hu, T., Ma, L. and Lin, Z. (2007), "Active vibration control for uncertain time varying systems via output feedback", *IEEE American Cont. Conf.*, July.
- Ikeda, T. (1996), *Fundamentals of Piezoelectricity*, Oxford University Press, New York.
- Kim, B., Washington, G.N. and Yoon, H.S. (2013), "Active vibration suppression of a 1D piezoelectric bimorph structure using model predictive sliding mode control", *Smart Struct. Syst.*, **11**(6), 623-635.
- Kugal, V. D. and Cross, L.E. (1998), "Behavior of soft piezoelectric ceramics under high sinusoidal electric fields", *J Appl. Phys.*, **84**(5), 2815-2830.
- Li, S., Zhao, R., Li, J., Mo, Y. and Zhenyu, S. (2014), "DOB-based piezoelectric vibration control for stiffened plate considering accelerometer", *Smart Struct. Syst.*, **14**(3), 327-345.
- Li, J. and Narita, Y. (2014), "Reduction of wind induced vibrations of a laminated plate with an active constrained layer", *J. Vib. Control*, **20**(6), 901-912.
- Lin, C.Y. and Chan, C.M. (2013), "Hybrid proportional derivative/repetitive control for active vibration control of smart piezoelectric structure", *J. Vib. Control*, **19**, 992-1003.
- Lin, C.C. and Huang, H.N. (1999), "Vibration control of beam and plates with bonded piezoelectric sensors and actuators", *Comput. Struct.*, **73**, 239-248.
- Malgaca, L. and Karagulle, H. (2009), "Simulation and experimental analysis of active vibration control of smart beams under harmonic excitation", *Smart Struct. Syst.*, **5**(1), 55-68.
- Masys, A.J., Ren, W., Yang, G. and Mukherjee, B.K. (2003), "Piezoelectric strain in lead zirconate titanate ceramics as a function of electric field, frequency and DC bias", *J Appl. Phys.*, **94**(2), 1155-1162.
- Petyt, M. (1998), *Introduction to Finite Element Vibration Analysis*, (2nd Ed.), Cambridge University Press, New York.
- Raja, S., Sinha, P.K., Partap, G. and Bhattacharya, P. (2002), "Influence of one and two dimensional piezoelectric actuation on active vibration control of smart panels", *Aerosp. Sci. Technol.*, **6**(3), 209-206.
- Sharma, M., Singh, S.P. and Sachdeva, B.L. (2005), "Fuzzy logic based modal space control of a cantilevered beam instrumented with piezoelectric patches", *Smart Mater. Struct.*, **14**(5), 1017-1024.
- Sharma, M., Singh, S.P. and Sachdeva, B.L. (2007), "Modal control of a plate using fuzzy logic controller", *Smart Mater. Struct.*, **16**(4), 1331-1341.
- Shin, C., Hong, C. and Jeong, W.B. (2013), "Active vibration control of beams using filtered velocity feedback controllers with moment pair actuators", *J. Sound Vib.*, **332**(12), 2910-2922.
- Sirohi, J. and Chopra, I. (2000), "Fundamental behavior of piezoceramic sheet actuators", *J. Intel. Mat. Syst. Str.*, **11**(1), 47-61.
- Smittakorn, W. and Heyliger, P.R. (2000), "A discrete-layer model of laminated hygrothermopiezoelectric plates", *Mech. Compos. Mater.*, **7**(1), 79-104.
- Wang, D., Fotinich, Y. and Carman, G.P. (1998), "Influence of temperature on electromechanical and fatigue behaviour of piezoelectric ceramics", *J. Appl. Phys.*, **83**(10), 5342-5350.
- Wang, Q.M., Zhang, T., Chen, Q. and Du, X.H. (2003), "Effect of DC bias field on complex materials coefficients of piezoelectric resonators", *Sensor. Actuat. A- Phys.*, **109**(10), 149-155.
- Zabihollah, A., Sedaghati, R. and Ganesan, R. (2007), "Active vibration suppression of smart laminated beams using layer wise theory and optimal control strategy", *Smart Mater. Struct.*, **16**(6), 2190-2201.
- Zenz, G., Berger, W., Nader M. and Krommer, M. (2013), "Design of piezoelectric transducer arrays for passive and active modal control of thin plates", *Smart Struct. Syst.*, **12**(5), 547-577.
- Zhang, Q.M., Wang, H. and Zhao, J. (1995), "Effect of driving field and temperature on the response behaviour of ferroelectric actuator and sensor materials", *J. Intel. Mat. Syst. Str.*, **6**(1), 84-93.
- Zhang, T., Li, H.G. and Cai, G.P. (2013), "Hysteresis identification and adaptive vibration control for a smart cantilevered beam by a piezoelectric actuators", *Sensor. Actuat. A- Phys.*, **203**, 168-175.